Fourier Transform Infrared and Raman Spectroscopic Study of Chromatographically Isolated Li@C 60 and Li@C 70

ARTICLE *in* THE JOURNAL OF PHYSICAL CHEMISTRY B · OCTOBER 2003

Impact Factor: 3.3 · DOI: 10.1021/jp030403w

5 AUTHORS, INCLUDING:

Andrey Gromov
The University of Edinburgh
37 PUBLICATIONS **583** CITATIONS
SEE PROFILE

Andreas Lassesson
Lund University
34 PUBLICATIONS **352** CITATIONS
SEE PROFILE

Martin Jönsson-Niedziolka
Polish Academy of Sciences
51 PUBLICATIONS **518** CITATIONS
SEE PROFILE

E. E. B. Campbell
The University of Edinburgh
322 PUBLICATIONS **7,435** CITATIONS
SEE PROFILE

Fourier Transform Infrared and Raman Spectroscopic Study of Chromatographically Isolated Li@C_{60} and Li@C_{70}

Andrei Gromov,* Denis Ostrovskii, Andreas Lassesson, Martin Jönsson, and Eleanor E. B. Campbell

Department of Experimental Physics, Göteborg University and Chalmers University of Technology, Göteborg, SE-41296, Sweden

Received: March 31, 2003; In Final Form: July 11, 2003

IR and Raman investigations have been carried out on purified Li@C_{60} and Li@C_{70} produced by low-energy ion implantation. The structural interpretations, based on theoretical considerations and comparison of the obtained vibrational spectra with those of different known fullerene oligomers, have shown that neither of the chromatographically isolated endohedral species (Li@$C_{60(70)}$) correspond to monomeric nonderivatized molecules. We ascribe the two different fractions of Li@C_{60} to a double-bonded dimer and a trimer, presumably with the shape of closed triangle. The infrared and Raman spectra of the Li@C_{70} compound are similar to those of $(C_{70})_2$, and we therefore propose for this species the structure of a double-bonded dimer $(Li@C_{70})_2$. The IR spectra of the Li@C_{60} fractions prepared with ^{6}Li and ^{7}Li isotopes are identical except for the position of broad bands at about 450−600 cm^{-1}, originating from vibrational−rotational movement of the Li^+ cation inside the carbon cage.

1. Introduction

Endohedral metallofullerenes, species with guest metal atom(s) encapsulated inside the fullerene cage, have been known for more than a decade. Much information is available concerning their production and properties, and speculations have been made concerning possible applications in various fields, such as nanoelectronics and material and biological sciences. The major aspects of endohedral metallofullerene research and applications have recently been comprehensively reviewed by Shinohara.[1]

The conventional method of endohedral fullerene production is arc-discharge or laser vaporization of graphite, impregnated with a metal compound. This method, in general, yields a variety of $M_x@C_n$ species (M = metal, $x = 1-3$, $n \geq 72$), which can be dissolved and further isolated from the fullerene-containing soot. M@C_{60} species are also formed during the arc-discharge process. According to mass-spectrometric analysis of the raw fullerene-containing soot, their production yields can significantly exceed those of soluble $M_x@C_n$ species.[2] However, contrary to endohedral metallofullerenes with higher cages, M@C_{60} complexes are not extractable from the soot by "normal" fullerene solvents, such as toluene or carbon disulfide. Some authors explain such behavior by formation of adducts and polymers due to the small highest occupied molecular orbital−lowest unoccupied molecular orbital (HOMO−LUMO) band gap[3] and decreased kinetic stability.[4] The formation of M@C_{60} endohedrals with a fullerene cage not satisfying the isolated-pentagon rule may also be possible during arc-discharge production and may be an additional explanation of their increased reactivity. However, several types of M@C_{60} have been successfully extracted from soot by pyridine[5] and aniline[6] or after surface modification to form metallofullerols.[7] The efficacy of pyridine and aniline can be explained, perhaps, by reversible formation of amine−metallofullerene adducts (charge-transfer complexes or derivatives with chemical bond formation) similarly to reactions with empty C_{60}.[8]

The number of genuinely isolated and investigated M@C_{60} species, produced by the arc-discharge method, is limited to only a few examples (M = Er,[9] Eu,[10] Dy,[11] and probably Gd[12]). Neeb et al.[13] succeeded in obtaining individual M@C_{60} (M = La, Ce) molecules that were isolated by in situ deposition of mass-selected plasma-generated metal−carbon clusters. However, the described method is not suitable for bulk production.

The alternative method of low-energy ion bombardment of fullerene films allows the production of bulk amounts of endohedral fullerenes that are confined to one specific fullerene cage.[14] The method is particularly suitable for synthesis of alkali-containing C_{60} and C_{70}. A high production efficiency can be reached using Li^+ ions for implantation. Because of its small radius, Li^+ (∼0.7 Å) easily penetrates the carbon cage with a threshold energy of about 5 eV. The highest production efficiency has been achieved for an ion energy of 30 eV and high ion current (5−10 μA).[14] However, at higher currents or ion energies beyond about 50 eV, there is an increasing tendency for polymerization of the bombarded fullerene film to occur. For energies higher than 70 eV, cage destruction becomes significant. This leads to a decrease in the amount of soluble endohedral fullerene material that can be extracted. To produce films of Li-containing fullerenes that can be further dissolved and purified, we generally use an ion/fullerene ratio of 1:1 at 30 eV ion energy, that typically gives about 10% yield of endohedral fullerenes.

High-performance liquid chromatographic (HPLC) analysis of ^{7}Li-bombarded C_{60} films shows that apart from the unreacted C_{60} two new fractions appear, both giving mass peaks at 727 u in laser desorption mass spectra (LDMS),[15] corresponding to the mass of LiC_{60}. Applying the same low-energy ion bombardment procedure to C_{70} films results in only one soluble product, which shows a mass peak at 847 u (LiC_{70}) in LDMS.[15,16] Photoionization and photofragmentation experiments on en-

* Corresponding author. E-mail: gromov@fy.chalmers.se.

10.1021/jp030403w CCC: $25.00
Published on Web 09/24/2003

riched Li@C_{60}[17] showed that the material could be evaporated intact and that, under appropriate laser excitation conditions, the decay of Li@C_{60} to Li@C_{58} by loss of C_2 ("shrink-wrapping") could occur in competition with the loss of Li from the cage.

Despite the availability of macroscopic amounts of material, it has proved difficult to obtain results from "bulk analysis" methods such as NMR and electron spin resonance (ESR) that could provide an unambiguous identification of the two Li@C_{60} and single Li@C_{70} fractions and incontrovertible proof of the endohedral nature of the material. This is partly due to the difficulty in handling the reactive material. In this paper we present structural evidence from infrared and Raman spectroscopic studies of chromatographically purified Li@C_{60} and Li@C_{70} species that provide an additional explanation for the difficulty of obtaining convincing ESR results. The spectroscopic evidence points to the oligomeric structure of the two purified fractions. In agreement with earlier assumptions,[15,18] the first fraction to be eluted is shown to be an endohedral dimer. The second fraction is now assigned to be an endohedral trimer rather than a monomer as earlier assumed. The interpretations are based on theoretical considerations and comparison of the obtained spectra with those of different known fullerene oligomers produced by various methods.

2. Experimental Details

The production and isolation of Li@C_{60} from unreacted C_{60} and other byproducts have been described elsewhere.[15,19] The fullerene film after low-energy ion bombardment was washed from the substrate by carbon disulfide (CS_2) in an ultrasonic bath. The CS_2-soluble part was examined by HPLC using a Cosmosil 5PBB column (Nacalai Tesque), 10 mm i.d., 25 cm length, and 1,2-dichlorobenzene as eluent at a flow rate of 2.5 mL/min. Except for the pure C_{60} fraction, two other components with different retention times were found (further denoted as E1 and E2, see Figure 1). Both new compounds show pronounced peaks at 727 u in their laser desorption time-of-flight (LD TOF) mass spectra (nanosecond N_2 laser desorption), corresponding to the mass of LiC_{60}, in agreement with earlier results.[15] LD TOF mass spectrometry can only give a lower limit for the amount of endohedral Li@C_{60} in any given sample because there is a strong propensity for loss of the Li from the cage at the high laser excitations needed for such studies.[17] From mass spectrometry studies using very low laser excitation and fast detection, this lower limit is on the order of 80% Li@C_{60} content for the two endohedral fractions. The results are similar for Li@C_{70}. Typically the mass ratio of E1/E2 species after isolation is equal to 1:2.

C_{120}, the [2 + 2] dimer of C_{60}, was prepared according to Lebedkin et al.[20] by mechanochemical reaction involving ball-milling of solid C_{60} in the presence of metallic lithium, followed by HPLC separation. The LD mass spectrum of the thus-obtained $(C_{60})_2$, measured under the same conditions as for Li@C_{60}, does not show any mass peak at 727 u, thus ensuring that the soluble part of the reaction mixture does not contain lithiated species (Li:C_{60} or Li@C_{60}).

Figure 1 shows typical chromatograms of CS_2-soluble parts of C_{60} and C_{70} films after bombardment with Li^+ ions at 30 eV compared to the Li−C_{60} dimerized material after ball-milling. The first endohedral fraction, Li@C_{60}-E1, arrives at a time that is very close to the elution time of pure $(C_{60})_2$. However, close inspection shows that the retention time for the Li-containing species is slightly longer, implying that it is indeed a different chemical compound. Similarly, the elution time of the second

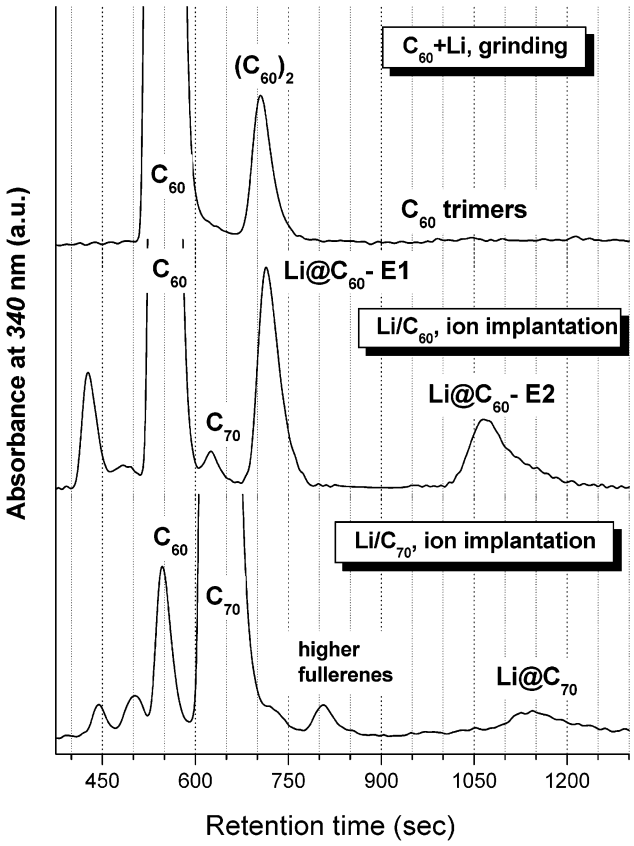

Figure 1. Typical chromatograms (Cosmosil 5PBB column, 1,2-dichlorobenzene eluent): (bottom) of the CS_2-soluble part of C_{70} film after low-energy bombardment with Li^+ ions; (middle) of the CS_2-soluble part of C_{60} film after low-energy bombardment with Li^+ ions; (top) of the 1,2-dichlorobenzene soluble part of Li/C_{60} material after ball-milling.

endohedral fraction, Li@C_{60}-E2, overlaps with that of $(C_{60})_3$ isomers but appears as an intense and rather narrow peak, quite different from the form of the pure trimer. The isolation of Li@C_{70} was carried out in the same way; however, in this case only one endohedral product was found (Figure 1). This result is in perfect agreement with previously reported data.[15,16] The peak marked "higher fullerenes" was confirmed to be this by LDMS and HPLC/UV−vis comparison with fullerene soot extract.

The purity of the separated Li@C_{60}-E1 and -E2 fractions was found to be ≥90%, as determined by HPLC analysis.

For this study we prepared Li@C_{60} samples containing both ^{7}Li and ^{6}Li isotopes, to be able to distinguish between the fullerene cage vibrations and vibrations due to the Li atom interaction with the C_{60} cage.

Infrared measurements were performed using a Bruker 22 Fourier transform infrared (FTIR) spectrometer (model Vektor) placed inside a glovebox with a dry argon gas atmosphere. The HPLC purified species (≥1 mg for Li@C_{60} species, ∼1 mg for Li@C_{70}) were additionally washed with methylene chloride to remove impurities and droplet-coated on KBr substrates under the flow of inert gas. The spectra were recorded at room temperature; spectral resolution was set to 2 cm^{-1} in all cases. A total of 15 000 scans were collected for the ^{6}Li@C_{60}-E2 and ^{7}Li@C_{60}-E2 fractions in order to increase the signal-to-noise ratio, while for other samples we used 500−1000 scans.

Fourier transform (FT) Raman spectra were recorded in a backscattering geometry at ambient conditions. The setup was a Bruker IFS-66 spectrometer equipped with a Raman module

FRA-106, a liquid-nitrogen-cooled Ge detector, and a Nd:YAG laser operating at a wavelength of 1064 nm. Each spectrum presented in this work is a result of 9−16 h of accumulation at a spectral resolution of 2 cm^{-1}, with a laser intensity of 20−40 mW, focused in the spot (∼100 W/cm^{-2}).

3. Results and Discussion

The unperturbed C_{60} molecule with I_h point group symmetry has 174 internal vibrations distributed between 46 distinct modes, of which only 4 are infrared active ($4F_{1u}$) and 10 are Raman active ($2A_g + 8H_g$). The reduction of the molecule's symmetry from, for example, doping, polymerization, etc., will result in a frequency shift of already existing spectral components, splitting of degenerate bands, and activation of previously inactive (silent) modes. Thus the location of a metallic cation M^+ at a particular site of the C_{60} cage will reduce the cage symmetry from the initial I_h as follows: M^+ at a pentagon site results in D_{5d} symmetry; M^+ at a hexagon site results in D_{3d} symmetry; M^+ at a double bond site results in C_{2v} symmetry.

However, according to density functional calculations of Li@C_{60}, charge transfer from Li to the cage occurs in such a way that the cation is trapped on a spherically symmetric potential with a minimum at 1.35−1.5 Å from the cage center, with a fairly homogeneous charge density distribution over the cage at room temperature.[21−23] At 300 K the lithium cation is essentially free to move on a "sphere" of this potential, and in this case the overall cage symmetry will not be significantly different from the original I_h configuration. The IR spectrum of such a compound will show four F_{1u} bands, originating from cage vibrations, and the motion of Li^+ inside the cage will be seen as a broad vibration−rotation band at 300−450 cm^{-1} with the overtone at 650−850 cm^{-1}.[21] Similarly, calculations[24b] predict that the Raman spectra of endohedral M@C_{60} (M = Li, Na, K) will be very similar to that of pristine C_{60}, that is, still containing only 10 bands but with some frequency shifts with respect to C_{60}.

A second consideration, which may lead to the reduction of the molecular symmetry, is the formation of cage-derivatized species during doping. Any stabilization of the unpaired cage electron by formation of a chemical bond, for example, by hydrogenation or dimerization, reduces the initial symmetry of the fullerene cage, with a corresponding influence on the vibrational spectra. The formation of dimers has been reported for exohedrally doped RbC_{60}[25,26] and RbC_{70}[27] materials, as well as for the isoelectronic $C_{59}N$ [28] and $C_{69}N$ [29] azafullerenes. For all these species, group-theoretical analysis predicts a large number of active vibrational modes (about 300). Although the real spectral traces contain "only" several tens of the bands from more than 300 predicted,[30] the spectrum of the dimer is considerably more complex than that of the monomer.

The overall spectral picture becomes more complicated for C_{70} compounds because the C_{70} molecule (D_{5h} symmetry group) has 204 normal vibrations, which produce 31 infrared and 53 Raman bands.[31] In addition, it has been shown that C_{70} may form five stable isomeric dimers[32−34] with different symmetry representations and, accordingly, should demonstrate different spectral features. Thus, similar to the situation for C_{60}, the analysis of experimentally reported spectra shows that dimerization causes a pronounced alteration of the vibrational spectra,[32] whereas exohedral doping does not significantly change the spectral profiles.[27]

On the basis of the above considerations, when analyzing the vibrational spectra of endohedral metallofullerenes, one may expect significant spectral changes due to the formation of fullerene derivatives and rather small spectral variations due to the metal cation doping of the fullerene cage.

3.1. Vibrational Spectra of Li@C_{60} Species. Figure 2 compares the middle IR spectra of the E1 and E2 fractions of Li@C_{60} with that of the C_{60} [2 + 2] dimer. The exact peak positions are collected in Table 1 along with assignments based on known literature data. It may be immediately noted from Figure 2 that the spectra of both endohedral phases differ significantly from that of pristine C_{60} (which shows only four peaks) but closely resemble the spectrum of the $(C_{60})_2$ dimer. Most of the bands in the spectra of the endohedrals and the dimeric phase are coincident, although a local variation of the relative intensities between the closely situated peaks is observed. However, in the infrared spectra of Li@C_{60} materials, five new well-resolved components appear at 746, 1034, 1376, 1455, and 1699 cm^{-1} (marked with arrows in Figure 2A). The band at 746 cm^{-1} could perhaps be explained by the splitting of the strong 4-fold degenerate $F_{2u}(2)$ mode of C_{60} (738 cm^{-1}) in $(C_{60})_2$ and the lithiated compounds; however, the presence of a sharp intense peak in the Li@C_{60} compounds suggests the presence of a new spectral component in this region. The other four bands are not observed at all in the spectra of the C_{60} monomer and dimer. Therefore, we ascribe these five modes to cage distortion by the endohedral Li^+ ion. We note here that such assignment is in qualitative agreement with ab initio calculations of Andreoni and Curioni,[35] where the appearance of new absorption peaks in the spectrum of Li@C_{60} has been noted at approximately the same frequencies. Moreover, the peak at 1376 cm^{-1} may be associated with a theoretically predicted band at ∼1350 cm^{-1},[35] which was found to be a characteristic feature for endohedral Li@C_{60} and did not appear in the exohedral compound.

When the infrared spectra of the E1 and E2 lithiated fractions are compared, several differences may be seen. Generally, the spectrum of E2 appears to be less distinct than that of E1, especially in the regions of 900−1300 cm^{-1} and 1500−1650 cm^{-1}. In addition, various splittings of the $F_{1u}(1)$- and $F_{1u}(2)$-derived modes at 526 and 576 cm^{-1}, respectively, may be noted (Figure 2B). For Li@C_{60}-E1 we observe a triplet splitting for the $F_{1u}(2)$ and $F_{1u}(1)$ modes. In these characteristic regions the spectrum looks quite similar to that of $(C_{60})_2$, but small differences in relative peak intensities are clearly observed. In addition, the spectrum of the E1 endohedral shows a new triplet group of peaks centered at about 550 cm^{-1}, which may be interpreted as being due to the activation of the previously silent $H_u(2)$ mode of C_{60} because of symmetry reduction.[36,37] In contrast, for Li@C_{60}-E2 we found a quadruplet splitting of the $F_{1u}(1)$ and $F_{1u}(2)$ modes as well as the appearance of the new H_u-related bands around 550 cm^{-1}. In the range of 600−900 cm^{-1} the peaks in Li@C_{60}-E1 and Li@C_{60}-E2 appear at approximately the same positions, implying that they are derived from the same newly activated modes of C_{60} (F_{2u}, G_u, and H_u).

Figure 3A shows the Raman spectra of Li@C_{60}-E1 and -E2 species in comparison with $(C_{60})_2$. The exact peak positions for all compounds are listed in Table 1. Similarly to the situation for infrared absorption, it is immediately seen that the spectra of the endohedral compounds match the spectrum of the C_{60} dimer much better than that of the monomer (which exhibits only 10 bands—two nondegenerate A_g modes and eight 5-fold degenerate H_g modes). However, in contrast to the infrared absorption, no principally new features are noted in the Raman spectra of the lithiated compounds. The main differences between the spectra of $(C_{60})_2$ and the endohedrals are observed in the low-frequency region (240−500 cm^{-1}), characteristic for

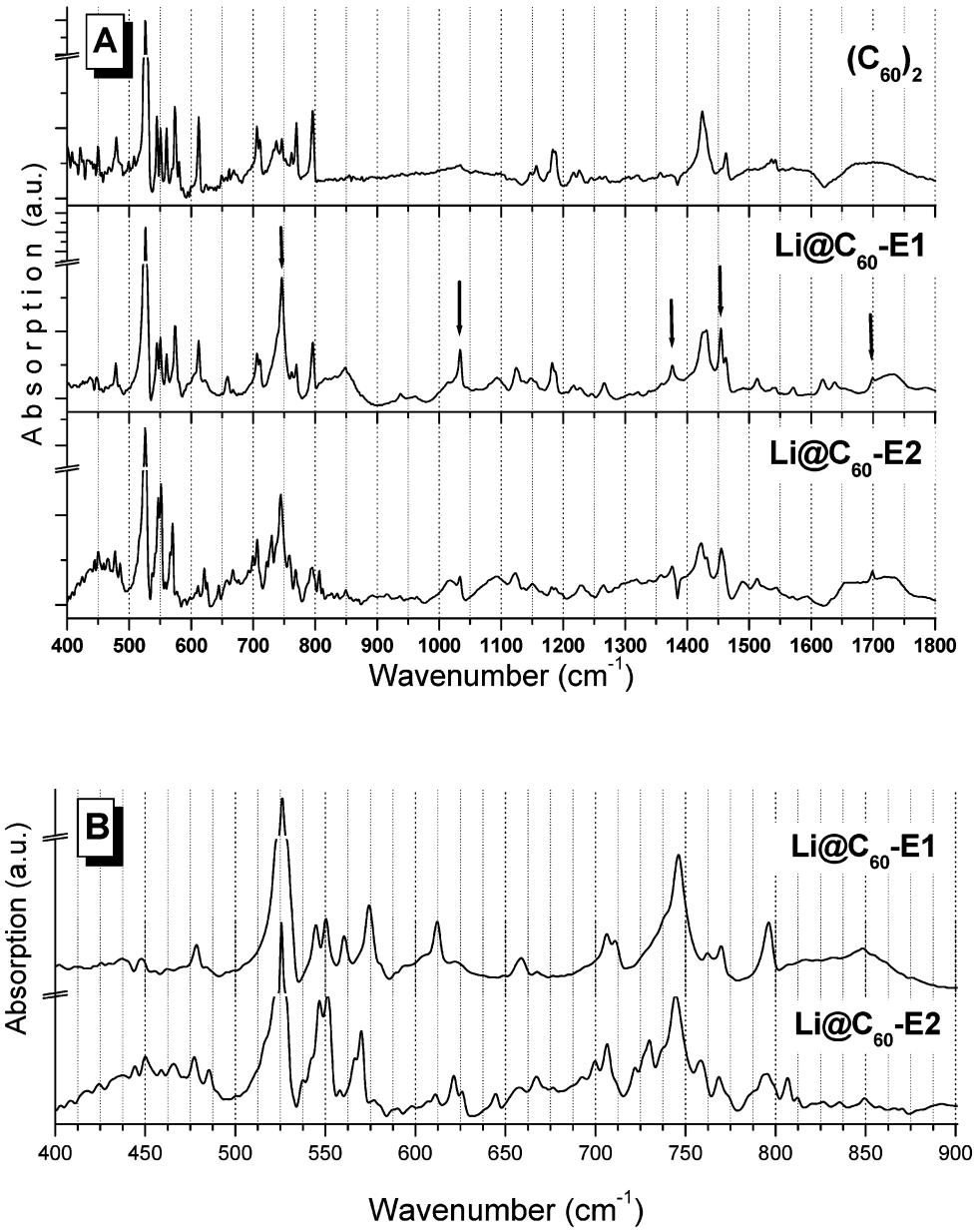

Figure 2. (A) Comparison of middle FTIR spectra of two chromatographically isolated Li@C_{60} fractions (as indicated). The spectrum of $(C_{60})_2$ is shown for comparison. (B) Expansion of the low-frequency region. Arrows mark spectral bands arising because of lithium insertion.

the radial modes of the C_{60} cage, and in the characteristic envelope of the pentagonal pinch mode ($A_g(2)$) around 1465 cm^{-1} (Figure 3B). Again, it is seen that the spectrum of the E1 fraction is quite similar to that of $(C_{60})_2$, and the only noticeable change is the split of the radial breathing mode ($A_g(1)$) at 490 cm^{-1} into two components of comparable intensity centered at 488 and 493 cm^{-1}. Such behavior is quite uncommon because the radial breathing mode is usually affected only slightly by doping or by covalent derivatization of the C_{60} cage.[38] At the same time, the $A_g(2)$ mode, which is known to be very sensitive to the charge on the cage (exhibiting a shift to low frequencies of about 6−9 cm^{-1} for each extra electron[38,39] and for covalent bonding[20,40]), only demonstrates a small downshift (1−1.5 cm^{-1}). In general, the investigation of the Raman peak splitting and intensities with respect to the $H_g(1)$ and $A_g(1)$ modes shows a high similarity between the doubly bonded C_{60} [2 + 2] dimer and Li@C_{60}-E1 with, however, some shifts in line positions. Such a similarity of the vibrational spectra along with the HPLC retention times strongly supports the assumption about the dimeric nature of Li@C_{60}-E1 species.

As for the infrared spectrum, the Raman spectrum of the E2 fraction looks more complex than the E1 fraction in terms of the number of components. This can be attributed to an overall lower molecular symmetry of the second endohedral species. In comparison with E1, the spectrum of E2 shows an additional splitting of the $H_g(1)$ mode at 271 cm^{-1} and broadening of the $H_g(8)$ mode around 1575 cm^{-1} (see Figure 3). Unfortunately, we could not investigate the region specific for the fullerene dimer intercage vibration modes because of a very strong broad band in the range below 120 cm^{-1} (with the center at ca. 60 cm^{-1}). This band is only observed for the endohedral compounds and could be due to the rotational motion of the Li inside the cage that is predicted to lie in this region.[24a] Other Raman evidence for internal Li motion has been discussed previously;[18] however, the intensity is rather low, and it is difficult to make any quantitative conclusions from the signal.

Detailed comparison of the spectral regions of interest (Figure 3B) shows three specific variations. First, the pentagonal pinch mode ($A_g(2)$) shifts toward lower frequency by 5 cm^{-1} (in comparison with the $(C_{60})_2$ dimer). Then, the radial breathing

TABLE 1: Infrared and Raman Bands Observed in Endohedral Li@C_{60} Compared to Those of C_{60} and $(C_{60})_2$

Infrared					Raman				
mode[a]	C_{60}	$(C_{60})_2$	Li@C_{60}-E1	Li@C_{60}-E2	mode	C_{60}	$(C_{60})_2$	Li@C_{60}-E1	Li@C_{60}-E2
$H_g(2)$		450	439, 448 vw	445, 450	Inter-			164.5, 174	160-200 w,br
		474.5 sh		467	cage			206.5, 214	
$G_g(1)$		479	479	477			252 sh	255 s	254, 247 sh
$A_g(1)$		487sh		486 vw			260 s		260s
		499			$H_g(1)$	271	271 s	269	274 m, 279 sh
		508		517 sh	$H_g(1)$[b]		297 m	296	296 s
$F_{1u}(1)$	526	526.5 vs	527	526 s	$H_u(1)$		310-395	340	331 vw
$F_{2g}(1)$		545	545	547			vvw	350w	
		551	551	551.5	$G_u(1)$		403 vw	393w	402 vw
$F_{1g}(1)$		560.5	560.5	566.5	$H_g(2)$	432	431 m-w	429	
		570vw	570	570	$H_g(2)$[b]		452 m-w	451	
$F_{1u}(2)$	576	574	574		$G_g(1)$		474.5 sh		
		580.5vw	581 w				479 s	488	486 m
$H_u(2)$		612		612 vw	$A_g(1)$	496	490, 501 w	492	
				622, 626,		515	520 m	515 w	512, 516 m
		649,661,		645, 657,	$F_{1u}(1)$	527	531 sh		520-540 w,br
		670 vvw		667 vw		557	551,555vw		
				700	$F_{1g}(1)$[b]		564 vw		
$H_u(3)$		706	706	706.5	$F_{1u}(2)$		574 vw		
$H_u(3)$		711	711	722, 726sh			627 w	608 vw	
				730	$A_g(2)$		1426, 1440		
$F_{2u}(2)$		738	739 sh	737.5 sh		1468	1463 vs	1462 s	1459 s
		746.5	746	744.5 m			1490 w		1466 sh
$G_u(2)$		762	762	759	$G_u(6)$		1520 w		
		770	770	767			1564 m		
$F_{2g}(2)$		796	796.5	795	$H_g(8)$	1574	1573 m	1571	1550-1605 br
$H_g(4)$			815, 849 br	807			1585 vw		
$F_2u(3)$			937vw	850 vw					1625 w, br
			962 vw						
$G_g(2)$			1010 w, br						
			1034 m	1034 m-w					
			1094 w, br	1094 m, br					
A_u[b]			1124 w	1123.5					
		1148,1157,	1149, 1154 vw	1151.5					
		1176,1184,	1183						
$F_{1u}(3)$	1183	1188	1189 w	1189					
		1217	1217						
$H_u(5)$		1227 vvw	1230 vw	1230					
			1266, 1376	1266					
$F_{1u}(4)$	1429	1424	1426	1423					
		1431, 1439	1431	1432					
		1456 vvw	1453	1455					
$A_g(2)$		1463	1462	1461 sh					
				1491,					
$F_{2g}(4)$[b]		1537,		1513,					
		1542 vvw		1544,					
				1594 vw					
				1655 br					
				1700 m					
				1736.5 br					

[a] Band assignment on the basis of refs 30, 31. [b] Mode of fcc C_{60}.

mode (~490 cm^{-1}) demonstrates the same frequency shift of 5 cm^{-1} and, moreover, undergoes a dramatic intensity decrease. Finally, in the low-frequency region (240−310 cm^{-1}), characteristic for squashing modes of C_{60}, we observe the appearance of a large number of modes and a noticeable intensity redistribution between different spectral components. It should be stressed that the observed behavior of the pentagonal pinch and low-frequency modes is very particular. In the comprehensive theoretical study of Porezag et al.[41] using the DF-TB method, Raman spectra of different C_{60} trimers were generated. The calculations show that while the species with linear, L-shaped, and open-triangle configurations generate characteristic envelopes for the low-frequency and pentagonal pinch modes, similar to those of the dimer, the C_{60} trimer with the geometry of a closed triangle will produce the following specific features (see Figures 3 and 4 in ref 41): (i) the pentagonal pinch mode keeps its single-band profile but is noticeably shifted toward lower frequencies; (ii) the 260−270 cm^{-1} double peak splits into several components in such a way that the relative intensity of the 260 and 296 cm^{-1} modes becomes the same. All these peculiarities are clearly observed in the Raman spectrum of the Li@C_{60}-E2 fraction. This is in agreement with the HPLC retention time for E2 (Figure 1) which falls into the region of C_{60} trimers.

Thus, from a general analysis of the vibrational spectra and the HPLC behavior, it may be concluded that neither of the chromatographically isolated endohedral Li@C_{60} species corresponds to the monomeric nonderivatized Li@C_{60}, which should exhibit a rather simple spectrum. On the basis of specific spectral peculiarities, we assign the E1 and E2 fractions to the endohedrally doped dimeric and trimeric forms of C_{60}, respectively. This finding does not contradict the LD TOF MS results, which show for both fractions pronounced peaks at 727 u, corresponding to monomeric LiC_{60}. It has been shown that

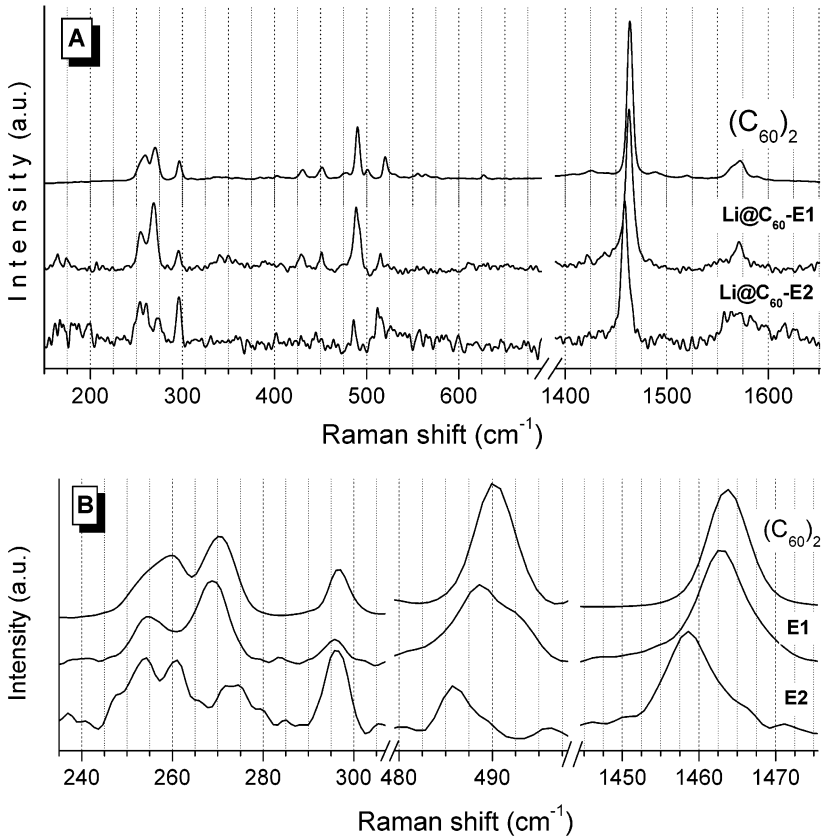

Figure 3. (A) Comparison of Raman spectra of two chromatographically separated Li@C_{60} fractions (as indicated). The spectrum of $(C_{60})_2$ is shown for comparison. (B) Expansion of the spectra in low-frequency, radial breathing, and pentagonal pinch mode characteristic regions.

isolated endohedral Li@C_{60} species possess limited thermal stability,[19] and they undergo complete dissociation of the interfullerene bonds under the rather extreme LD MS conditions. The same problem occurs for other dimeric species, for example, $(C_{60})_2$ [42] and $(C_{70})_2$.[32]

A more detailed analysis of the structures of both endohedral species will be given in following sections.

To uncover the cage modes most sensitive to the Li^+ insertion, we carried out the synthesis of Li@C_{60} species doped with the ^{6}Li isotope. According to density functional calculations,[21] Li^+ ion motion inside the C_{60} cage, governed by a "reflected Morse" potential, should reveal itself as a broad band-head structure at 350 cm^{-1} and, possibly, by a first overtone at 700 cm^{-1}. Accordingly, for ^{6}Li-containing materials these bands must be shifted by 30−60 cm^{-1} toward higher frequencies. The appearance of such a broad absorption band in the range of 400−530 cm^{-1} has been previously reported for as-produced ^{7}Li:C_{60} films, before HPLC isolation of CS_2-soluble species.[43] Infrared spectra of ^{7}Li@C_{60}-E2 and ^{6}Li@C_{60}-E2 endohedral fractions are presented in Figure 4. It is clearly seen that the positions and the relative intensities of cage modes for both compounds are in general coincident, with some minor exceptions. It is important to note that the specific infrared bands that appeared in ^{7}Li@C_{60}-E2 because of Li^+ insertion (734, 1034.5, 1455, 1699 cm^{-1}; see Table 1) are also observed in the spectrum of ^{6}Li-doped material, with practically the same relative intensities. Because neither of these bands shows frequency variation, it may be concluded that these new modes arise because of Li-induced changes of the cage symmetry and that in the middle infrared range there are no absorption peaks originating solely from the vibrations involving Li−C interaction. This is in good agreement with theoretical simulations, which predict fast quasi-free motion of the Li^+ ion inside the C_{60} cage.[22, 23]

Thus, the only visible difference between the FTIR spectra of ^{6}Li and ^{7}Li endohedrals should become apparent in the position of the broad bands, arising from rotation−vibration movement of the Li atom inside the fullerene cage. The infrared traces of both isotopically substituted materials contain clearly pronounced broad-band structures (marked by arc-lines in Figure 4), which overlap with the peaks arising because of cage vibrations. The first low-frequency band (fundamental vibration−rotation band[21]) appears at 400−550 cm^{-1} for ^{7}Li@C_{60} and exhibits a clear shift to higher frequencies by about 50 cm^{-1} on ^{7}Li → ^{6}Li substitution (Figure 4). A similar behavior can be assumed for the first overtone vibration−rotation band (marked by dashed lines): the center of gravity of the broad bands shifts from ∼700 to ∼770 cm^{-1} with ^{7}Li → ^{6}Li substitution. However, in this case the overlap with multiple cage vibration modes at 650−820 cm^{-1} hampers the analysis of the band structure.

3.2. Vibrational Spectra of Li@C_{70}. The IR and Raman spectra of chromatographically isolated Li@C_{70} are shown in Figures 5 and 6, respectively, along with the reference spectra of $(C_{70})_2$.[32] The exact peak positions are listed in Table 2. As for the case of C_{60}-based materials, the IR spectrum of Li@C_{70} is more similar to that of $(C_{70})_2$ (Figure 5), especially in the intervals of 500−700 cm^{-1} and 1350−1500 cm^{-1}. However, the lithiated compound exhibits specific absorption peaks, which are not observed in the pure dimer, at 734, 745, 1015, and 1253 cm^{-1} as well as a new group of peaks at 950−1100 cm^{-1}. We especially note the presence in the spectrum of the peak at 745 cm^{-1}, which was also a fingerprint in the spectra of both Li@C_{60} phases. It is important to stress that, while in the C_{60} materials the 746 cm^{-1} peak could be assigned to the splitting of the F_{2u}-(2) mode (738 cm^{-1}), in the case of Li@C_{70} the 734−745 cm^{-1} double band is obviously a new feature appearing because of lithium insertion. In addition, in the frequency envelope of 400−

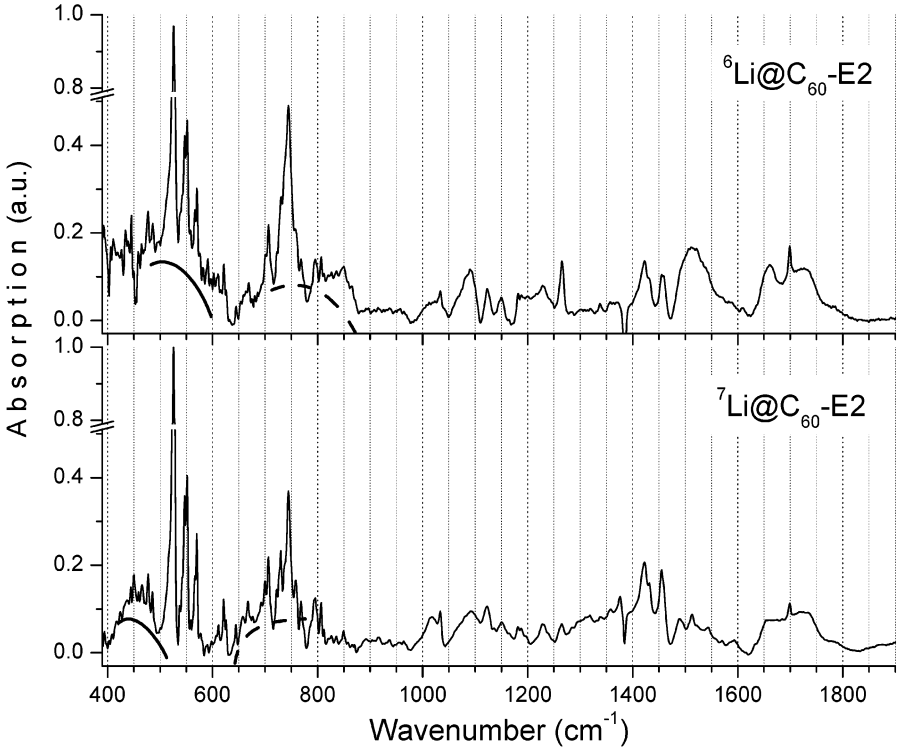

Figure 4. FTIR spectra of HPLC-isolated Li@C_{60}-E2 fractions produced by low-energy bombardment with ^{6}Li and ^{7}Li isotopes. The arc-lines show the underlying absorption bands assigned to the vibration−rotation motion of Li inside the C_{60} cage.

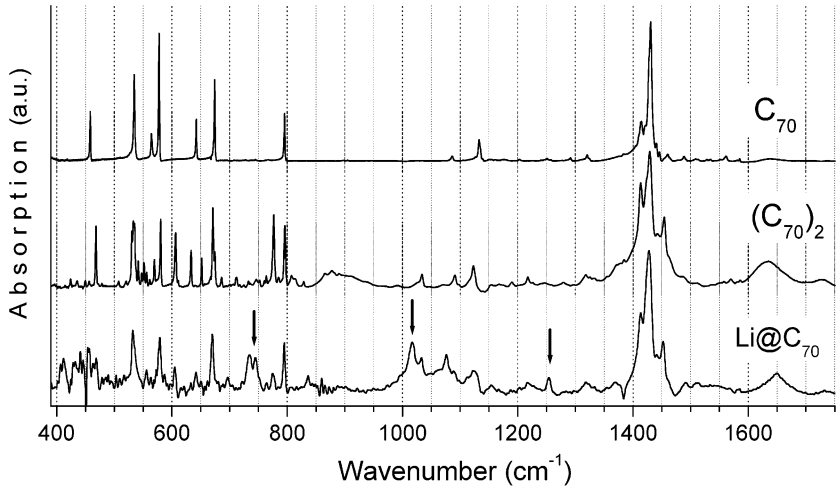

Figure 5. Comparison of the FTIR spectrum of chromatographically purified Li@C_{70} with the spectra of the C_{70} monomer and dimer. Arrows mark spectral bands arising because of lithium insertion.

500 cm^{-1} the presence of a wide absorption band, underlying the sharp spectral peak, is suggested. Similarly to the C_{60} based endohedral, the increase of absorption in this spectral region may be ascribed to the Li motion inside the fullerene cage. We note, however, that in the IR spectrum of Li@C_{70} this feature cannot be clearly resolved. In general, the IR spectrum of Li@C_{70} looks more complex in terms of the number of modes than that of $(C_{70})_2$, which can be evidence of symmetry reduction in Li@C_{70} with respect to the C_{2h} symmetry of the C_{70} [2 + 2] dimer.[32]

The assumption concerning the dimeric nature of the chromatographically purified Li@C_{70} species is confirmed by a noticeable resemblance between the Raman spectra of Li@C_{70} and $(C_{70})_2$ (Figure 6). Both substances show a similar splitting and shift of the original C_{70} modes. However, with respect to $(C_{70})_2$, Li@C_{70} demonstrates a redistribution of band intensities and more complex line splittings, especially in the range 1100−1600 cm^{-1}, and clearly exhibits a downshift (by 2−5 cm^{-1}) of several modes. The latter may result from the additional negative charging of the C_{70} cage in Li@C_{70}. Thus, the comparison of the vibrational spectra strongly suggests that chromatographically isolated Li@C_{70} exists in the form of dimer(s), and similarly to the C_{60}-based materials, no presence of endohedrally doped nonderivatized monomer may be detected.

3.3. Structure of Endohedral (Lithiated) Dimers. As discussed above, the main products formed by low-energy ion bombardment of fullerene films and isolated by HPLC are very likely lower oligomers of Li@$C_{60/70}$. In this section we will perform a detailed comparison of the experimental vibrational spectra of the investigated materials with the known literature data in order to draw out certain conclusions about the structural peculiarities of the samples under study.

3.3.1. Dimer of Li@C_{60}. A number of $(C_{60})_2$ species have been studied theoretically, including a single-bonded dimer,

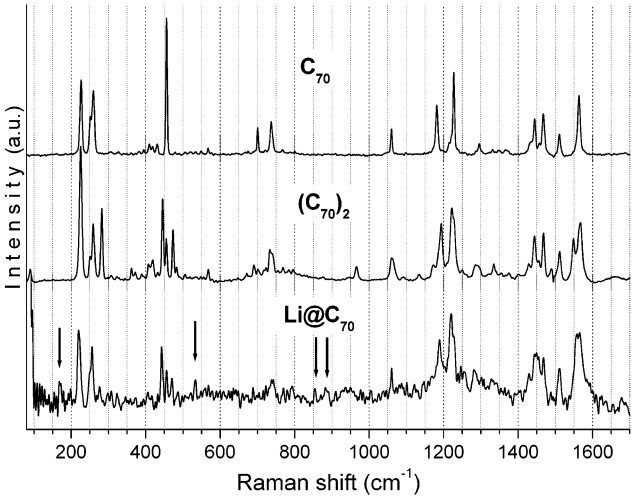

Figure 6. Comparison of Raman spectrum of chromatographically isolated Li@C_{70} with the spectra of C_{70} monomer and dimer. Arrows mark spectral bands arising because of lithium insertion.

various isomers of $(C_{60})_2$ formed by [2 + 2] cycloaddition, peanut-type structures, several types of C_{120} "cages" (isomers of C_{120} fullerene), and tubelike molecules (e.g., refs 44 and 45). The formation of fullerene-like "cage", "tube", and "peanut" structures, however, requires a large energetic barrier on the order of 85 eV to be overcome,[46] and they are thus unlikely to be formed in our experiments. Therefore, we will consider the possibility of formation of only two types of C_{60} dimers: the single-bonded and double-bonded ones.

Theoretical calculations show that the most stable conformation of neutral dimers, $(C_{60})_2$, is the (66/66) isomer of the [2 + 2] cycloadduct.[47] Such a dimer is believed to be formed during photopolymerization,[45,48] high pressure−temperature treatment,[30,32] and mechanochemical reactions.[20,42] In contrast, the single-bonded dimer of neutral C_{60} is reported to be quite unstable.[47] However, the situation is reversed in the case of negatively charged fullerene cages. Most of the theoretical calculations predict a slightly higher stability for the single-bonded anion dimer $(C_{60}^-)_2$ than for the double-bonded one.[47] This is confirmed experimentally for exohedrally doped fullerenes; for example, A_1C_{60} has been shown to produce single-bonded dimers.[25,26,38] Similarly, azafullerene, the $C_{59}N$ molecule isoelectronic to the C_{60}^- anion, forms a stable single-bonded dimer.[28] No evidence for the formation of negatively charged C_{60}^- double-bonded dimers has been reported so far.

It is instructive to note, however, that all energetic calculations on negatively charged cages are usually based on the consideration of the C_{60}^- properties and do not take into account any effect of the positive ion. In the exohedrally doped compounds a "single unit" of the material is comprised of a separate fullerene cage with a delocalized negative charge and an external localized positive charge (cation). Such a unit will form a dipole. In the endohedrally doped compounds a monomer unit is represented by a cage in which the delocalized negative charge will be compensated by the same delocalized positive charge inside the cage (i.e., by the cation moving around the geometric center of the cage).

It should be noted that the spectral behavior of $(C_{60}^-)_2$ and $(C_{60})_2$ dimers is expected to be rather similar. Group symmetry analysis predicts for the single-bonded (syn-conformer with C_{2v} symmetry) and double-bonded (D_{2h}) species close numbers of active bands: 174 IR and 174 R (single-bonded); 132 IR and 174 R (double-bonded). The number of experimentally observed peaks is lower than this; the weak intensity and strong overlap between the split components of the C_{60} degenerate modes hamper the detailed analysis, making an exact band assignment practically impossible. As discussed above, the infrared and Raman spectra of the Li@C_{60} endohedral fullerenes closely resemble the traces of pristine $(C_{60})_2$ (Figures 2 and 3) and agree well with the reported spectra of double-bonded dimers from photopolymerized[48] and high pressure−temperature-treated C_{60}.[30] On the other hand, the spectra of the exohedrally doped Rb_1C_{60} dimeric phase[26] and the $(C_{59}N)_2$ molecule,[38,49] which are composed of units isoelectronic to Li@C_{60} and known to form single-bonded dimers, also show similar spectral features. The infrared spectrum of the negatively charged dimer $(C_{60}^-)_2$ shows a splitting of the $F_{1u}(1)$, $F_{1u}(2)$, and $F_{1u}(4)$ bands, a triplet splitting of the $F_{1u}(3)$ peak, and the appearance of a number of new modes in the 600−900 and 1200−1600 cm^{-1} intervals.[26] $(C_{59}N)_2$ shows a splitting pattern almost coincident with that of $(C_{60}^-)_2$ for all F_{1u} modes in IR and H_g modes in the Raman spectra and exhibits differences only for C−N-related bands and a higher frequency of the $A_g(2)$ mode around 1460 cm^{-1}.[38] Thus, the vibrational spectra of single- and double-bonded C_{60} dimers are quite close to each other, and it is difficult to find a critical difference between these species on the basis of a comparison in general terms. However, there are some significant differences. For instance, in a detailed comparative study of the Raman spectra of several types of C_{60} dimers, Plank et al.[38] have reported that, despite a great common similarity, the spectra of single-bonded dimers (both $(C_{60}^-)_2$ and $(C_{59}N)_2$) demonstrate strong bands at about 448 and 625 cm^{-1} assigned, respectively, to the $G_g(1)$ and $G_g(2)$ modes, which do not appear in the spectrum of the neutral double-bonded $(C_{60})_2$ dimer. In the Raman spectrum of the $(C_{60})_2$ species obtained by high-temperature−high-pressure treatment, only a weak feature at 450 cm^{-1} has been observed[30] (assigned to the $H_g(2)$ mode of C_{60}); the spectrum of the C_{60} dimer obtained by mechanochemical preparation[20] also did not reveal any significant bands in the regions of interest. Thus it can be concluded that the strong Raman bands around 448 and 625 cm^{-1} are unique fingerprints of the single-bonded C_{60} dimers.

Another specific difference between single- and double-bonded C_{60} dimers can be found in their infrared spectra. In the theoretical modeling of the IR spectra of different neutral $(C_{60})_2$ isomers,[44] it has been found that the "dumbbell" structure should produce two characteristic bands dealing with the atomic motions localized around the intercage double bond. The combination of these modes produces a single peak in the infrared spectrum centered at about 875 cm^{-1}. However, taking into account the accuracy of the theoretical calculations and the predicted relative intensity of this band (∼25% of maximum), this mode has been tentatively ascribed to the peak at 793 cm^{-1} observed in the experimental spectra of Onoe et al.[48] Indeed, an absorption band of significant intensity at 795 cm^{-1} has been repeatedly noted for double-bonded dimers (in pressure-polymerized or photopolymerized C_{60}),[30,42,50] whereas it has never been observed in the spectra of single-bonded species (dimeric form of Rb_1C_{60} and $(C_{59}N)_2$).[26,49] Therefore the presence of this band in the infrared spectrum may be considered as a fingerprint of the double-bonded dimer.

Now let us analyze the experimental vibrational spectra of the dimeric Li@C_{60} compound (E1 fraction) in terms of the appearance of the characteristic bands. A close look at the infrared spectrum (see Figure 2A and Table 1) immediately shows the presence of a pronounced band centered at 796 cm^{-1}, which is practically identical in shape and intensity to the band observed in the spectrum of the neutral $(C_{60})_2$ dimer. The Raman

TABLE 2: Infrared and Raman Bands Observed in Endohedral Li@C_{70} Compared to Those of C_{70} and $(C_{70})_2$

Infrared				Raman			
mode[a]	C_{70}	$(C_{70})_2$	Li@C_{70}	mode	C_{70}	$(C_{70})_2$	Li@C_{70}
		424, 435.5	407, 412.5			88.5 vw	169.5 w
		450	416 sh	E_2'	228.5 s	222.5	220.5
				E_1''	252.5 m	250	250
A_2''	458	456	425-475 w	A_1'	263	256	256
		468 s				298.5	
		507.5, 521		E_2''		310	
		530.5		E_1'		363	
E_1'		533		E_2''	383	374	
E_1''	535	535	533			390	
		537.5 sh		A_1'	396	395	
A_2'		541.5, 547, 551	540 sh,			407	
E_1''		556.5	556	E_1''	410.5	411	
E_2''	564	561.5	564	E_1'	420	420	
A_2''	566 sh	569.5 m		E_2'	432.5	432	
A_1'	578	580 s	579, 588			445 s	443, 448 sh
E_1'		606 s	606	A_1'	457 s	456	456
		611w,		E_2'	500	472.5 m	464 vw
						484	470, 487 w
		630.5 sh		A_1'	568	568	533.5
		633.5 m		E_1'	578		
E_1'	642.5	651.5 m	642 w	E_2'	669		
		667		E_1''	677		
				A_1'	702 m		
		671 s	671	E_2'	721 vw	718, 724	
E_1'	674	674.5 m	697.5 w			733	
E_2'		686	722 w	E_2'	738 m	743	740 w,br
		712	735, 745		763		
		746, 752	754 sh	E_2'	768	769	
		760, 764	764.5,	E_1'		796	
		776.5 s	775	E_1''	802	802	854 w
		785		E_2'		945	886 w
E_1'	795.5	796 s	795 s			968 m	
		807.5		A_1'	1061 m	1060	1060.5
		813.5 w,br				1065	1050-1113 br
		829, 866	837	E_2''		1073 sh	
A_1''		878, 889				1136	
A_2'		913 br				1172	
		937 br		A_1'	1184.5 m	1190	1189
		1025 br	1018	E_2'			
		1034	1033.5	A_2'	1215 sh		1220.5
E_1'	1086.5	1091	1076, 1090.5 w	E_1''	1221 sh	1223	1227.5
		1116.5 sh	1114	A_1'	1228 s	1231 sh	
	1124 w	1123	1125	E_2'	1257	1250.5	
A_2''	1133 s				1288	1286,1290	1285 br
E_2''	1150 w			E_1''	1296.5	1298	
	1154 w		1156 w,br	E_1'		1325 w	
E_1'	1161			E_2'	1333	1335	1334 br
E_1''	1176 w,br	1190				1342 sh	
A_2''	1203 w	1217	1220 w,br	E_2'	1350	1356	
A_1''	1240			E_1''	1368	1370 w,br	
E_1'	1246			E_2	1375	1400	
	1250.5		1255	E_1'		1407	
E_2'	1254 sh					1423 sh	1429
	1257.5			E_1'	1435	1431	
E_1'	1284						
	1289 sh						
E_1'	1292			E_1''	1445.5 m	1444.5	1450
E_1''	1309			A'	1458	1456	
E_2''	1314			A_1'	1469 m	1469	1468
E_1'	1320.5 m	1318	1321 w,br			1492	
A_2''	1324	1326, 1332				1505 sh	
	1384 vw	1380 br		E_1''	1512 m	1512.5	1511
E_1'	1410	1413 s	1414	A_1''		1550	1557.5
	1421	1423 m-s	1425	E_2''	1564 m	1563	1565
E_1'	1427	1429 s		A_1'		1570	1600 sh,br
	1430.5						
A_2'	1440.5vw	1442 m	1443				
E_1''	1446 vw	1454	1453				

TABLE 2 (Continued)

Infrared				Raman			
mode[a]	C_{70}	$(C_{70})_2$	Li@C_{70}	mode	C_{70}	$(C_{70})_2$	Li@C_{70}
E_1'	1477.5	1464 m					
	1481.5						
	1484.5 sh						
E_1'	1489 m		1492				
	1492,1497						
	1503 sh						
	1506 sh						
	1508						
E_1''	1512.5		1513				
E_2''	1528.5						
	1534.5						
A_1''	1551.5						
A_2''	1559						
E_1'	1562						
	1566						
E_2'	1585						
	1638 m,br	1635 br, 1729 w,br	1651 br				

[a] Band assignment on the basis of ref 31.

TABLE 3: Correlation between Specific Vibrational Modes Observed in the Spectra of Different C_{60} Dimers[a]

	$(C_{60}^-)_2$		$(C_{59}N)_2$		$(C_{60})_2$						Li@C_{60} (E1)
ν (cm^{-1})[b]	ref 38	ref 26	ref 38	ref 49	ref 38	ref 20, 48	ref 48	ref 30	ref 47	this work	this work
448 (R)	s	na[c]	s	na[c]	—[d]	—[d]	na[c]	—[d]	na[c]	—[d]	—[d]
625 (R)	vs	na[c]	m	m	—[d]	—[d]	na[c]	—[d]	na[c]	—[d]	—[d]
795 (IR)	na[c]	—[d]	na[c]	—[d]	na[c]	na[c]	s	m-s	s	s	m

[a] Lettering for intensities is standard. [b] Frequency position varies slightly (±2 cm^{-1}) in different works. [c] Not available. [d] Not observed.

spectrum (Figure 3), in turn, does not contain any pronounced bands around 448 and 625 cm^{-1}. Table 3 summarizes the presence or absence of spectral signatures in the spectra of the different types of C_{60}-based dimers. By comparison of the characteristic spectral features of the various systems, it can be immediately concluded that the Li@C_{60} material corresponds to a double-bonded species. It should be stressed that a double-bonded Li@C_{60} dimer would not be in contradiction with calculations, which predict very close total energies for $(C_{60}^-)_2$ isomers with double- and single-intercage bonds.[47]

The assignment of the infrared absorption peak at 796 cm^{-1} to the characteristic mode of the intercage-related vibration in the double-bonded dimer has additional support from the comparison of the infrared spectra of the two endohedral Li@C_{60} fractions E1 and E2. This band is much less clearly defined in the trimer (E2) spectrum compared to that in the dimer (E1). In the case of the trimer the band at 796 cm^{-1} splits into a series of low-intensity components (Table 1). Considering the type of vibrations responsible for this band, it appears that the main contribution is given by the motion of the atoms nearest to the intercage bridge in the plane of the double bond (upper plot in Figure 7).[44] In the optimized structure of the "closed-triangle" trimer[41] (bottom plot in Figure 7) all three intercage linkages sit in the same plane. This implies that the atoms of each C_{60} in such a trimer, located between neighboring intercage linkages, will be forced to move in different directions simultaneously. As a result, about half of the atoms contributing to the 796 cm^{-1} band are practically excluded from the vibrations. Consequently, this band will split and lose overall intensity—the situation which is clearly observed in the spectrum of the E2 fraction.

3.3.2. Dimer of Li@C_{70}. In the case of C_{70}-based materials the situation is less certain. The possible structures of a neutral $(C_{70})_2$ dimer have been studied and discussed in the literature. Five isomers, representing different [2 + 2] cycloadditions across the short double bond, with similar energies of formation

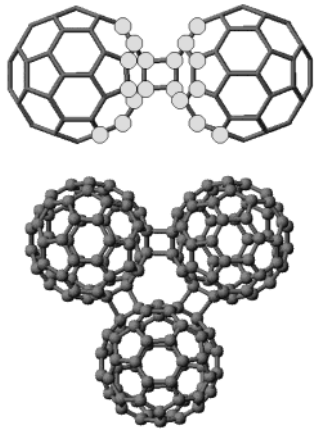

Figure 7. (Top) Double-bonded C_{60} dimer. Circles mark the atoms which are strongly involved in the vibrations producing the infrared absorption band at 796 cm^{-1}. (Bottom) Optimized structure of the C_{60} trimer with the closed-triangle geometry (from ref 41).

but different orientations of the monomers relative to the intercage bridge are possible.[32−34] Therefore it is quite difficult (if possible at all) to establish an exact structure of C_{70}-based dimer complexes solely on the basis of the vibrational spectra.

When it comes to the charged C_{70} species, and especially their dimers, the situation is even more difficult because of the lack of experimental investigations. To our knowledge, only a few publications dealing with $(C_{70}^-)_2$ complexes are available.[27,51,52] Neutron scattering and Raman spectra of exohedrally doped Rb_1C_{70} suggested the formation of charged C_{70}^- dimers.[27,51] This phase appeared to be much more stable than the C_{60}-based analogue: it demonstrated perfect stability up to 400 K, and even at 500 K its signatures were still observed.[27] Under further heating, the Rb_1C_{70}-based dimer dissociated in favor of C_{70} monomers and did not form a polymer compound like Rb_1C_{60}.[27,51] Such different properties were attributed by the authors to the

electronic peculiarities of the C_{70} cage in comparison with C_{60}. On the basis of the similarity of the neutron scattering spectra of Rb_1C_{60} and Rb_1C_{70}, it has been suggested that the $(C_{70}^-)_2$ dimer has a single-bonded structure. At the same time, the Raman spectrum of the Rb_1C_{70}-based dimer was practically identical to that of pure C_{70},[27] and no characteristic band splitting in isolated neutral $(C_{70})_2$ [32] and in materials under investigation (see Figure 5) were observed.

Taking into account the fact that the vibrational spectra of chromatographically isolated Li@C_{70} show specific features characteristic for the neutral $(C_{70})_2$ dimer, we may assume that the material exists in the form of lithiated dimers $(Li@C_{70})_2$, and no monomeric form of the endohedral compound or oligomers higher than the dimer can be concluded to be present. The intercage bond order remains an open question, but in analogy with the C_{60} material, a double-bonded compound would seem the most likely candidate.

4. Summary and Conclusions

The chromatographically isolated fractions of Li@C_{60} and Li@C_{70} metallofullerenes produced by low-energy ion bombardment were analyzed by infrared and Raman spectroscopy. Two distinct Li@C_{60} fractions with different retention times and one single Li@C_{70} fraction were separated from the bombarded fullerene films by HPLC. In the solid state, the investigated compounds demonstrated no signs of structural variation (decomposition or polymerization) over a period of months at room temperature. The results of a comprehensive spectroscopic study and careful comparison of the experimental vibrational spectra with those reported in the literature for relevant fullerene monomers and dimers showed the following:

(1) Neither of the isolated endohedral species obtained by low-energy ion bombardment corresponds to the monomeric nonderivatized doped molecule (Li@$C_{60(70)}$). The Li@C_{60} fraction with the shorter retention time (E1) may be ascribed to a double-bonded dimer of endohedral Li@C_{60}. The fraction with a longer retention time (E2) may be ascribed to the lithiated C_{60} trimer, presumably with the shape of a closed triangle. The infrared and Raman spectra of the Li@C_{70} compound are similar to those of $(C_{70})_2$, and we therefore propose for this species the structure of a double-bonded dimer $(Li@C_{70})_2$.

(2) Insertion of a Li^+ ion inside the fullerene cage (for both C_{60} and C_{70}) results in activation of vibrational modes, which are not observed in the spectra of exohedral monomers and dimers. Comparison of IR spectra of Li@C_{60}-E2 species produced with ^{6}Li and ^{7}Li isotopes shows that there are no peaks due to the interaction between the trapped cation and the carbon cage—a result that agrees well with known calculations. Therefore we tentatively ascribe new bands to the lowering of the molecular symmetry of the doped compounds in comparison to the pristine ones.

(3) The endohedral nature of the materials was evident through the presence of specific features that can be identified as vibration−rotational bands originating from Li^+ motion inside the carbon cage. In the spectra of endohedral C_{60}-based compounds it was observed as an appearance of broad underlying infrared absorption bands in the spectral regions of 400−500 and possibly 650−750 cm^{-1} (for ^{7}Li-doped samples), with a high-frequency shift of about 50−70 cm^{-1} in the ^{6}Li-based materials. Unfortunately, the relatively low intensity of these bands and their strong overlap with the strong modes of the cage vibrations do not allow a more exact determination of the band parameters.

Acknowledgment. The authors are indebted to Dr. Sergei Lebedkin (University Karlsruhe/Forschungszentrum Karlsruhe, Germany) for providing the experimental IR and Raman data files for $(C_{70})_2$[32] used in this work for comparison with the endohedral fullerene spectra. A.G., A.L., and M.J. thank the EU FET-IST program for financial support within the NICE project. D.O. thanks Vetenskapsrådet (Sweden) for financial support.

References and Notes

(1) Shinohara, H. *Rep. Prog. Phys*. **2000**, *63*, 843.

(2) (a) Guo, T.; Diener, M. D.; Chai, Y.; Alford, J. M.; Haufler, R. E.; McClure, S. M.; Ohno, T. R.; Scuseria, G. E.; Smalley, R. E. *Science* **1992**, *257*, 1661. (b) Moro, L.; Ruoff, R. S.; Becker, C. H.; Lorents, D. C.; Malhorta, R. *J. Phys. Chem.* **1993**, *97*, 6801.

(3) Diener, M. D.; Alford, J. M. *Nature* **1998**, *393*, 668.

(4) Aihara, J. *Phys. Chem. Chem. Phys.* **2001**, *3*, 1427.

(5) (a) Kubozono, Y.; Ohta, T.; Hayashibara, T.; Maeda, H.; Ishida, H.; Kashino, S.; Oshima, K.; Yamazaki, H.; Ukita, S.; Sagabe, T. *Chem. Lett*. **1995**, 457. (b) Kubozono, Y.; Noto, T.; Ohta, T.; Maeda, H.; Kashino, S.; Emura, S.; Ukita, S.; Sagabe, T. *Chem. Lett*. **1996**, 453.

(6) (a) Kubonozo, Y.; Maeda, H.; Takabayashi, Y.; Hiraoka, K.; Nakai, T.; Kashino, S.; Emura, S.; Ukita, S.; Sagabe, T. *J. Am. Chem. Soc*. **1996**, *118*, 6998. (b) Kubonozo, Y.; Hiraoka, K.; Takabayashi, Y.; Nakai, T.; Ohta, T.; Maeda, H.; Ishida, H.; Kashino, S.; Emura, S. *Chem. Lett*. **1996**, 1061. (c) Takabayashi, Y.; Kubozono, Y.; Hiraoka, K.; Inoue, T.; Mimura, K.; Maeda, H.; Kashino, S. *Chem Lett*. **1997**, 1019.

(7) Wilson, L. J.; Cagle, D. W.; Thrash, T. P.; Kennel, S. J.; Mirzadeh, S.; Alford, J. M.; Ehrhardt, G. J. *Coord. Chem. Rev*. **1999**, *190*−*192*, 199.

(8) Skiebe, A.; Hirsch, A.; Klos, H.; Gotschy, B. *Chem. Phys. Lett*. **1994**, *220*, 138.

(9) Inoue, T.; Kubozono, Y.; Kashino, S.; Takabayashi, Y.; Fujutaka, K.; Hida, M.; Inoue, M.; Kanbara, T.; Emura, S.; Uruga, T. *Chem. Phys. Lett*. **2000**, *316*, 381.

(10) Ogawa, T.; Sugai, T.; Shinohara, H. *J. Am. Chem. Soc*. **2000**, *122*, 3538.

(11) Kanbara, T.; Kubozono, Y.; Takabayashi, Y.; Fujiki, S.; Iida, S.; Haruyama, Y.; Kashino, S.; Emura, S.; Akasaka, T. *Phys. Rev. B* **2001**, *64*, 113403.

(12) Bolskar, R. D.; Alford, J. M.; Benedetto, A. F.; Husebo, L. O.; Wilson, L. I. *Abstracts of Papers*, 223rd National Meeting of the American Chemical Society, Orlando, FL, April 7−11, 2002; American Chemical Society: Washington, DC, 2002.

(13) Neeb, M.; Klingeler, B.; Bechthold, P. S.; Kann, G.; Wirth, I.; Eisebitt, S.; Eberhardt, W. *Appl. Phys. A* **2001**, *72*, 289.

(14) Tellgmann, R.; Krawez, N.; Lin, S.-H.; Hertel, I. V.; Campbell, E. E. B. *Nature* **1996**, *382*, 407.

(15) Gromov, A.; Krätschmer, W.; Krawez, N.; Tellgmann, R.; Campbell, E. E. B. *Chem. Commun*. **1997**, 2003.

(16) Krawez, N.; Gromov, A.; Tellgmann, R.; Campbell, E. E. B. *AIP Conf. Proc.* **1998**, *442* (Electronic Properties of Novel Materials—Progress in Molecular Nanostructures), 368.

(17) Rohmund, F.; Bulgakov, A. V.; Heden, M.; Lassesson, A.; Campbell, E. E. B. *Chem. Phys. Lett*. **2000**, *323*, 173.

(18) Gromov, A.; Krawez, N.; Lassesson, A.; Ostrovskii, D. I.; Campbell, E. E. B. *Curr. Appl. Phys.* **2002**, *2*, 51.

(19) Krawez, N.; Gromov, A.; Buttke, K.; Campbell, E. E. B. *Eur. Phys. J. D* **1999**, *9*, 345.

(20) Lebedkin, S.; Gromov, A.; Giesa, S.; Gleiter, R.; Renker, B.; Rietschel, H.; Krätschmer, W. *Chem. Phys. Lett*. **1998**, *285*, 210.

(21) Joslin, C. G.; Yang, J.; Gray, C. G.; Goldman, S.; Poll, J. D. *Chem. Phys. Lett*. **1993**, *208*, 86.

(22) Li, Y. S.; Tomanek, D. *Chem. Phys. Lett*. **1994**, *221*, 453.

(23) Campbell, E. E. B.; Fanti, M.; Hertel, I. V.; Mitzner, R.; Zerbetto, F. *Chem. Phys. Lett*. **1998**, *288*, 131.

(24) (a) Joslin, C. G.; Gray, C. G.; Goldman, S.; Yang, J.; Poll, J. D. *Chem. Phys. Lett*. **1993**, *215*, 144. (b) Leion, H. M.S. Thesis, Chalmers University of Technology, Göteborg, Sweden, 2002.

(25) (a) Oszlanyi, G.; Bortel, G.; Faigel, G.; Tegze, M.; Gránásy, L.; Pekker, S.; Stephens, P. W.; Bendele, G.; Dinnebier, R.; Mihály, G.; Jánossy, A.; Chauvet, O.; Forró, L. *Phys. Rev. B* **1995**, *51*, 12228. (b) Mehring, M.; Their, K.-F.; Rachdi, F.; de Swiet, T. *Carbon*, **2000**, *38*, 1625.

(26) Martin, M. C.; Koller, D.; Rosenberg, A.; Kendziora, C.; Mihaly, L. *Phys. Rev. B* **1995**, *51*, 3210.

(27) Schober, H.; Renker, B. *Solid State Commun*. **1997**, *104*, 609.

(28) Hummelen, J. C.; Knight, B.; Pavlovich, J.; Gonzalez, R.; Wudl, F. *Science* **1995**, *269*, 1554.

(29) (a) Tagmatarchis, N.; Okada, K.; Tomiyama, T.; Shinohara, H. *Synlett* **2000**, 1761. (b) Tagmatarchis, N.; Forman, G. S.; Shinohara, H. *AIP Conf. Proc.* **2001**, *591* (Electronic Properties of Molecular Nanostructures), 29.

(30) Davydov, V. A.; Kashevarova, L. S.; Rakhmanina, A. V.; Senyavin, V. M.; Ceolin, R.; Szwarc, H.; Allouchi, H.; Agafonov, V. *Phys. Rev. B* **2000**, *61*, 11936.

(31) (a) Schettino, V.; Paglai, M.; Cardini, G. *J. Phys. Chem. A* **2002**, *106*, 1815. (b) Brockner, W.; Menzel, F. *J. Mol. Struct.* **1996**, *378*, 147.

(32) Lebedkin, S.; Hull, W. E.; Soldatov, A.; Renker, B.; Kappes, M. M. *J. Phys. Chem. B* **2000**, *104*, 4101.

(33) Heine, T.; Zerbetto, F.; Seifert, G.; Fowler, P. W. *J. Phys. Chem. A* **2001**, *105*, 1140.

(34) Forman, G.; Tagmatarchis, N.; Shinohara, H. *J. Am. Chem. Soc.* **2002**, *124*, 178.

(35) Andreoni, W.; Curioni, A. *Appl. Phys. A* **1998**, *66*, 299.

(36) Wang, K.-A.; Rao, A. M.; Eklund, P. C.; Dresselhaus, M. S.; Dresselhaus, G. *Phys. Rev. B* **1993**, *48*, 11315.

(37) Long, V. C.; Musfeldt, J. L.; Kamaras, K.; Adams, G. B.; Page, J. B.; Iwasa, Y.; Mayo, W. E. *Phys. Rev. B* **2000**, *61*, 13191.

(38) Plank, W.; Pichler, T.; Kuzmany, H.; Dubay, O.; Tagmatarchis, N.; Prassides, K. *Eur. Phys. J.* **2000**, *17*, 33.

(39) (a) Wang, K.-A.; Wang, Y.; Zhou, P.; Holden, J. M.; Ren, S.; Hager, G. T.; Ni, H. F.; Eklund, P. C.; Dresselhaus, G.; Dresselhaus, M. S. *Phys. Rev. B* **1992**, *45*, 1955. (b) Zhou, P.; Wang, K.-A.; Wang, Y.; Eklund, P. C.; Dresselhaus, M. S.; Dresselhaus, G.; Jishi, R. A. *Phys. Rev. B* **1992**, *46*, 2595. (c) Winter, J.; Kuzmany, H.; Soldatov, A.; Persson, P.-A.; Jacobsson, P.; Sundqvist, B. *Phys. Rev. B* **1996**, *54*, 17486.

(40) Burger, B.; Winter, J.; Kuzmany, H. *Z. Phys. B* **1996**, *101*, 227.

(41) Porezag, D.; Jungnickel, G.; Fraunheim, Th.; Seifert, G.; Ayuela, A.; Pederson, M. R. *Appl. Phys. A* **1997**, *64*, 321.

(42) (a) Wang, G.-W.; Komatsu, K.; Murata, Y.; Shiro, M. *Nature* **1997**, *387*, 583. (b) Komatsu, K.; Wang, G.-W.; Murata, Y.; Tanaka, T.; Fujiwara, K. *J. Org. Chem.* **1998**, *63*, 9358.

(43) Krawez, N. Ph.D. Thesis, Freie Universität Berlin, Germany, 1999.

(44) Esfarjani, K.; Hashi, Y.; Onoe, J.; Takeuchi, K.; Kawazoe, Y. *Phys. Rev. B* **1998**, *57*, 223.

(45) Strout, D. L.; Murry, R. L.; Xu, C.; Eckhoff, W. C.; Odom, G. K.; Scuseira, G. E. *Chem. Phys. Lett.* **1993**, *214*, 576.

(46) Rohmund, F.; Glotov, A.; Hansen, K.; Campbell, E. E. B. *J. Phys. B* **1996**, *29*, 5143.

(47) (a) Pekker, S.; Oszlanyi, G.; Faigel, G. *Chem. Phys. Lett.* **1998**, *282*, 435. (b) Kürti, J.; Nemeth, K. *Chem. Phys. Lett.* **1996**, *256*, 119. (c) Scuseria, G. E. *Chem. Phys. Lett.* **1996**, *257*, 583.

(48) Onoe, J.; Takeuchi, K. *Phys. Rev. B* **1996**, *54*, 6167.

(49) Krause, M.; Baes-Fischlmair, S.; Pfeiffer, R.; Plank, W.; Pichler, T.; Kuzmany, H.; Tagmatarchis, N.; Prassides, K. *J. Phys. Chem B* **2001**, *105*, 11964.

(50) Rao, A. M.; Eklund, P. C.; Hodeau, J.-L.; Marques, L.; Nunez-Regueiro, M. *Phys. Rev. B* **1997**, *55*, 4766.

(51) Renker, B.; Schober, H.; Heid, R. *Appl. Phys. A* **1997**, *64*, 271.

(52) (a) Ren, A.; Feng, J.; Sun, X.; Li, W.; Tian, W.; Sun, C.; Zheng, X.; Zerner, M. C. *Int. J. Quantum Chem.* **2000**, *78*, 422. (b) Konarev, D. V.; Khasanov, S. S.; Vorontsov, I. I.; Saito, G.; Antipov, M. Yu.; Otsuka, A.; Lyobovskaja, R. N. *Chem. Commun.* **2002**, 2548.